Computational Fluid Dynamics JOURNAL vol.8 no.3 1999 (pp.400–409)

# COMPRESSIBLE VISCOUS FLOW PAST AEROFOILS USING A NON-OSCILLATORY FINITE-VOLUME SCHEME

S. B. HAZRA† S. K. CHAKRABARTTY‡ P. NIYOGI♯

Abstract

Theory of non-oscillatory schemes has been used in conjunction with a finite-volume cell-vertex Navier-Stokes solver in this paper, in order to compute compressible viscous flow fields past airfoils which accurately capture shock without preshock oscillations. The SLIP (symmetric limited positive) scheme with scalar splitting and with flux-difference splitting schemes proposed by Jameson(1993) have been implemented here, These schemes have the LED (local extremum diminishing) property which is equivalent to that of TVD (total variation diminishing) in one-dimension. Typical transonic test cases have been studied. It is found that both the schemes provide very good shock resolution at high Mach numbers for steady solution of the viscous fluid How equations expressed by Reynolds averaged Navier-Stokes equations in conservation law form augmented with Baldwin-Lomax (1978) turbulence model.

Key words: Non-oscillatory schemes, cell-vertex finite-volume, steady viscous flow, TVD, LED, transonic flow, supersonic flow, shock computation.

## 1 INTRODUCTION

Significant progress has been achieved in the past two decades in the area of numerical solution of Euler and Navier-Stokes equations. During eighties several second-order accurate shock-capturing schemes for solving Euler equations of gas dynamics were developed which could successfully and efficiently compute flow past complex configurations[1]-[5]. Among these, the finite-volume scheme of Jameson et. al.[1] became particularly popular due to its efficiency and robustness. It showed that steady-state flows containing moderately strong shock waves could be quite well predicted by a central difference scheme augmented by a carefully controlled blend of first, and third order dissipative terms. Works on numerical solution of Navier-Stokes equations followed soon [6]-[18].

During this period, several authors attempted to construct numerical schemes that could eliminate spurious preshock oscillations that appeared in the computational solutions. Further, algorithm development was aimed at combining high accuracy with high resolution of shocks and contact discontinuities.

It has long been recognized that first order upwind differencing like that of Godunov scheme[21] can eliminate spurious oscillations in the neighborhood of shock waves at the expense of low accuracy in regions where the flow is smooth. Central difference schemes on the other hand, produce good solutions in smooth regions but are prone to oscillations in the neighborhood of shock waves, which can be suppressed only by the introduction of additional dissipative terms.

Stemming from the mathematical theory of hyperbolic conservation laws [22], Harten[27] proposed the concept of total variation diminishing (TVD) finite-difference schemes and constructed such a second order scheme by introducing antidiffusive terms and flux limiters to improve shock resolution. Similar idea may be found in the work of Boris and Book[23]. TVD schemes preserve the monotonicity of an initially monotone profile, because the total variation would increase if the profile ceased to be monotone. Consequently they prevent spurious oscillations. Van Leer [24] used flux limiters to produce a second order accurate scheme which would preserve the monotonicity of an initially monotone profile. Important contributions on TVD schemes have been made by Roe[25],[26], Osher[28],[29], Yee[31],[32] and many of the ideas on

Received on February 3, 1999.

Department of Mathematics, Indian Institute of Technology; Kharagpur-721302, INDIA
† Present address: Centre for Mathematical Modelling and Computer Simulation (C-MMACS); Bangalore-560037, India,
‡ Scientist; Computational and Theoretical Fluid Dynamics Division, NAL; Bangalore, India
♯ Retired. Present address: 42A, Naskarpara Road, Santoshpur, Calcutta-700 075, India,

flux limiters have been unified by Sweby[30]. A survey of the other important works on TVD schemes for computational solution of Eulers equations may be found in Yee[32].

In a series of papers, Jameson[33]-[36] developed the theory of non-oscillatory schemes with particular reference to finite-volume space discretization with multi-stage time-stepping schemes for Euler equations of gas dynamics and to Navier-Stokes equations in [36]. TVD Navier-Stokes solution appear in Yee et.al. [37].

This paper presents application and implementation of flux limiters and LED (local extremum diminishing ) schemes, originally introduced by Jameson[35], in order to obtain high resolution of shock waves without preshock oscillations. Finite-volume cell-vertex discretization originally put forward by Chakrabartty [15] with algebraic turbulence model of Baldwin and Lomax[38] has been used in the present study. Steady-state viscous transonic flow past airfoils nave been computed using an algebraically generated C-type grid following Jain[39]. A multistage Runge-Kutta type of time-stepping has been used for time integration.

## 2 GOVERNING EQUATIONS

Two-dimensional Navier-Stokes equations in integral form representing conservation of mass, momentum and energy may be expressed in integral form as

$$\frac{\partial}{\partial t}\int_{\Omega}\vec{W}\partial\Omega+\int_{\partial\Omega}\overline{\overline{H}}_{E}.\vec{n}\,ds+\int_{\partial\Omega}\overline{\overline{H}}_{V}.\vec{n}\,ds=0 \quad (1)$$

for a fixed region $\Omega$ with boundary $\partial\Omega$. Here, $\vec{n}$ denotes the unit outward normal to $\partial\Omega$ and $\overline{\overline{H}}E$ and $\overline{\overline{H}}_V$ are the Eulerian and viscous flux vectors respectively. Here the body forces and heat sources have been neglected. In terms of the flow variables pressure $p$, density $p$, Cartesian velocity components $u$ and $v$, total energy $E$, absolute temperature T and total enthalpy $H$ per unit mass, the quantities $\vec{W}$, $\overline{\overline{HE}}$ and $\overline{\overline{H}}_V$ may be expressed as

$$\vec{W}=\begin{bmatrix}P\\ \rho u\\ \rho v\\ \rho E\end{bmatrix},\quad \overline{\overline{H}}_E=\begin{bmatrix}\rho\vec{q}\\ \rho u\vec{q}+p\vec{i}_x\\ \rho v\vec{q}+p\vec{i}_y\\ \rho H\vec{q}\end{bmatrix},$$

$$\overline{\overline{H}}_V=\begin{bmatrix}0\\ \overline{\overline{\tau}}.\vec{i}_x\\ \overline{\overline{\tau}}.\vec{i}_y\\ \overline{\overline{\tau}}.\vec{q}-\vec{Q}\end{bmatrix} \quad (2)$$

where, the velocity vector $\vec{q}$, the stress-tensor $r$ and heat flux $\vec{Q}$ are given by

$$\vec{q}=u.\vec{i}_x+v.\vec{i}_y,\quad \overline{\overline{\tau}}=\begin{bmatrix}\sigma_x & \tau_{xy}\\ \tau_{xy} & \sigma_y\end{bmatrix}, \quad (3)$$

$$\sigma_x=-\lambda\left(\frac{du}{\partial x}+\frac{\partial v}{\partial y}\right)-2\mu\frac{\partial u}{\partial x},$$

$$\sigma_y=-A\left\{\frac{\partial u}{\partial x}+\frac{\partial v}{\partial y}\right\}-2\mu\frac{du}{dy},$$

$$\tau_{xy}=\tau_{yx}=-\mu\left\{\frac{du}{\partial y}+\frac{dv}{\partial x}\right\}.$$

$$\vec{Q}=K\nabla T=K\left(\frac{\partial T}{\partial x}\vec{i}_x+\frac{\partial T}{\partial y}\vec{i}_y\right),$$

$$E=e+\frac{1}{2}\left(u^2+v^2\right),\quad H=E+\frac{p}{\rho}. \quad (4)$$

Here, $\vec{i}_x$, $\vec{i}_y$ are the Cartesian unit vectors and e is the specific internal energy. For a perfect gas the equation of state is

$$p=\rho RT \quad (5)$$

where $R = C_p - C_v$. The specific heats of the gas $C_p$ and $C_v$ are assumed to be constants. The quantities $\mu$ and A are the first and second coefficients of viscosity respectively. Here A has been taken to be $-2\mu/3$ (Stokes'hypothesis). Sutherland's law is used to relate p and the absolute temperature T. The coefficient of thermal conductivity $K$ has been evaluated assuming the Prandtl number to be constant and it is assumed to be unity here.

For turbulent flows, the Reynolds-averaged Navier-Stokes equations exhibit a term by term correspondence with their laminar flow counterparts, except that the stress tensor is augmented by the Reynolds-stress tensor and the heat flux vector is augmented by the additional turbulent heat flux. To close the time averaged equations in turbulent flow, the two layer algebraic eddy-viscosity model [38] has been used.

## 3 FINITE VOLUME SPATIAL DISCRETIZATION

In the present formulation, the generation of a body-fitted grid using curvilinear co-ordinates and the solution process are separated since no global transformation is used. The only required data concerning the grid are the Cartesian co-ordinates of the four vertices of every cell in the given mesh.

The computational domain is subdivided into a large number of quadrilateral cells ($\Omega_{ij}$) by joining the cell vertices by straight lines as shown in Fig.1. According to the present scheme the flow variables are

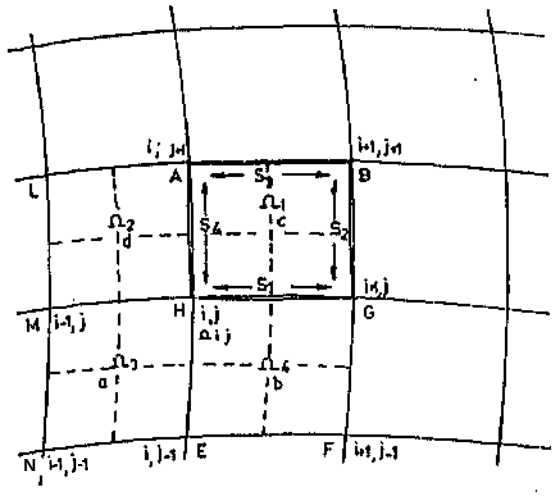


Fig.1: Finite volume mesh

defined at the nodal point $(i,j)$ and the fluxes are to be calculated across a control volume (abcd in Fig.l) formed by joining the centroids of the four neighbouring cell $\Omega_1$, $\Omega_2$, $\Omega_3$ and $\Omega_4$ (Fig.l). Since the conservation law, equation (1), is valid for any arbitrary control volume, it also holds locally for each cell $(\Omega_{ij})$.

Hence,

$$\frac{\partial}{\partial t}\int_{\Omega ij}\vec{W}d\Omega + \int_{\partial\Omega_{ij}}\overline{\overline{H}}_E.\vec{n}\,ds + \int_{\partial\Omega_{ij}}\overline{\overline{H}}_V.\vec{n}\,ds = 0 \tag{6}$$

where the boundary $\partial\Omega_{ij}$ consists of the four sides of the quadrilateral abcd, and $\vec{n}$ is the outward normal to the surface element $ds$. The volume $Vij$ of the cell fijj is computed by averaging the volumes of the four neighbouring ceils $\Omega_1$, fia> $\Omega_3$ and fi4 surrounding the point $(i,j)$. The discrete analog of equation(6) is written as

$$V_{ij}\left(\frac{d}{dt}\vec{W}_{ij}\right) + \vec{Q}_{ij} = 0, \quad \vec{Q}_{ij} = \vec{Q}_{E_{ij}} + \vec{Q}_{V_{ij}} \tag{7}$$

where $\vec{Q}_{E_{ij}}$ and $\vec{Q}_{V}$ represent the net inviscidand viscous fluxes out of a cell and is balanced by the rate of change of $\vec{W}_{ij}$.

The Eulerian fluxes have been calculated following a two stage scheme:

1. Flow quantities at the vertices of each cell are used to calculate the first order changes within the cell,
2. The first order changes in four neighboring cells are used to calculate the total change at the common, central vertex using the distribution formula

$$\frac{\partial}{\partial t}W|_H = \frac{X}{Y}.$$

$$X = Q_{E_{i,j}}V_{i,j} + Q_{E_{i-1,j}}V_{i-1,j} + Q_{E_{i,j-1}}V_{i,j-1} + Q_{E_{i-1,j-1}}V_{i-1,j-1}$$
$$Y = V_{i,j} + V_{i-1,j} + V_{i,j-1} + V_{i-1,j-1} \tag{8}$$

The value of the conserved variable representing a particular cell side has been obtained by averaging its values at the two corners.

First order changes due to viscous fluxes across $\Omega_{ij}$ have been calculated in the following way:

1. From the primitive values at the points H, G, B and A calculate the fluxes along the sides HG, GB, BA and AH (Fig.l). We use Green's theorem to get the first derivatives at the center c of the cell $\Omega_1$.
2. Calculate $\sigma_x$, $\tau_{xy}$, etc. at the centroids of the four neighbouring cells $\Omega_1, \Omega_2$, $\Omega_3$ and fi^.
3. Knowing $\sigma_x$, $\tau_{xy}$ etc. at a, b, c and d, calculate the viscous fluxes across ab, bc, cd and da.
4. Use Green's theorem to get the second derivatives from the net flux across the cell fi^j.
5. Add the viscous corrections at the vertex to the corresponding Euler corrections to update the flow variables.

The details of getting the derivatives and their order of accuracy may be found in [15].

## 4 BOUNDARY CONDITIONS

At a solid wall boundary, no-slip boundary condition is that both $u$ and $v$ velocity components are equal to zero and wall temperature is either prescribed or the normal derivative of the temperature is assumed to be zero (adiabatic wall). The surface boundary condition is implemented by placing fictitious image cells inside the body, needed for computing the first order derivatives at, the centre of the cells surrounding the control points for viscous fluxes. Boundary points coincide with the vertices of the cells where the flow variables are known. A simple extrapolation of the pressure to the vertices of the image cells is generally sufficient and both the velocity components are set antisymmetric.

An internal cut is required in the physical domain in order to make the computational domain simply connected. For this type of cut, periodic boundary conditions are implemented by forming image cells on both sides of the cut line and proper correspondence between the grid cells and the image cells is taken care of by specifying the image block, face and the orientation of the segment.

At the symmetry plane, boundary conditions are applied by adding dummy grid cells, and reflecting the values of the flow variables from the interior grid point to the dummy grid points.

The treatment of the farfield boundary is based on the concept of Riemann invariants for one dimensional inviscid flow normal to the boundary [1].

At an inflow boundary, the tangential velocity components and the entropy are prescribed from their free-stream values, while at an outflow boundary these values are extrapolated from the interior of the domain, as in Swanson and Turkel [11].

## 5 METHOD OF SOLUTION

The semi-discretization process discussed above completely separates the discretization of the space and time derivatives. The resulting system (7) of ordinary differential equations in time is solved using explicit five-stage Runge-Kutta time stepping scheme. Artificial dissipation terms are properly blended with natural viscosity for numerical stability. To accelerate the rate of convergence the local time stepping, enthalpy damping and residual smoothing have been applied [1].

### 5.1 Artificial Dissipation and Time Step Limit

The artificial dissipation terms used in the original scheme of Chakrabartty [13],[14] are based on Jameson et. al. [1]. However, a modified time step limit has been used, derived for a two-dimensional advection diffusion equation [19], [20], and summarized in this subsection. The finite-volume discretization described in the previous section amounts to central differencing and requires the addition of explicit dissipation terms for stability. Dissipative fluxes are added to the average flux $Q_{ij}$ in Eq.(7) to give

$$V_{ij}\left(\frac{d}{dt}\vec{W}_{ij}\right) + \vec{Q}_{ij} - \vec{D}_{ij} = 0 \qquad (9)$$

where $\vec{D}_{ij}$ is the artificial dissipative flux, and is given by

$$\vec{D}_{ij} = \vec{d}_{i+1/2,j} - \vec{d}_{i-1/2,j} + \vec{d}_{i,j+1/2} - \vec{d}_{i,j-1/2}. \qquad (10)$$

In the scheme of Jameson et. al.[1] $\vec{d}$ y are a special kind of blend of second and fourth order differences expressed by

$$\vec{d}_{i+1/2,j} = \alpha_{i+1/2,j}\left\{\epsilon^{(2)}_{i+1/2,j}\left(\vec{W}_{i+1,j} - \vec{W}_{i,j}\right)\right.$$
$$\left. -\epsilon^{(4)}_{i+1/2,j}\left(\vec{W}_{i+2,j} - 3\vec{W}_{i+1,j} + 3\vec{W}_{i,j} - \vec{W}_{i-1,j}\right)\right\} \qquad (11)$$

Here $\epsilon^{(2)}_{i+1/2}$ . and $\epsilon^{(4)}_{i+1/2}$ . are adaptive coefficients designed to switch on enough artificial dissipation where it is needed and are defined as

$$\nu_{i,j} = \frac{|\, p_{i+1,j} - 2p_{i,j} + p_{i-1,j}\,|}{p_{i+1,j} + 2p_{i,j} + p_{i-1,j}} \qquad (12)$$

$$\epsilon^{(2)}_{i+1/2,j} = k^{(2)} max(\nu_{i+1,j}, \nu_{i,j}) \qquad (13)$$

$$\epsilon^{(4)}_{i+1/2,j} = max\{0, (k^{(4)} - \epsilon^{(2)}_{i+1/2,j})\} \qquad (14)$$

and fc'2', $k^{(4)}$ are user specified constants, which control the artificial dissipation.

The scaling factor $\alpha_{i+1/2,j}$ is given by

$$\alpha_{i+1/2,j} = \frac{1}{2}\left(\frac{V_{i,j}}{\Delta t^*_{i,j}} + \frac{V_{i+1,j}}{\Delta t^*_{i+1,j}}\right) \qquad (15)$$

where $V_{i,j}$is the cell volume and $\Delta t^*_i$ • is an estimate of the time step limit for a nominal Courant number $(= c\frac{\Delta t}{\Delta x})$ of unity. The coefficient $\epsilon^{(2)}$ is proportional to the second difference of pressure in smooth regions of the flow proportional to the square of the mesh size, while $\epsilon^{(4)}$ is of order one. The quantity *pH* has been used instead of *pE* in the dissipative terms in the energy equation in order to admit $H$ = constant, a solution of that. Although physical dissipation is present in the equations, these may not be sufficient due to nonlinear effect, especially in the case of highly stretched meshes. On the other hand, the numerical dissipation should not overhelm the natural dissipation (i.e., the order of numerical dissipation should be higher than dissipation of the equation).

The value of $\Delta t^*_{i,j}$ used to calculate the scale factor $a$ in equation (15) was formulated on the basis of two-dimensional advection equation ([1]), which is appropriate for Euler equations where diffusive terms due to artificial dissipation were not significant for subsonic flows. For viscous flow computation using Navier-Stokes equations having strong pressure gradient, separation or shocks, it showed difficulties in reaching the steady state. In view of this, the scaling factor a has been modified by taking into account the time step limit for the advection diffusion equation [20]. The time step limit Ay at the point $(i, j)$, derived by satisfying the CFL condition, may be expressed as

$$\Delta_{ij} \le \Lambda_c \left[\frac{|A|\Delta y + |B|\Delta x}{\Delta x \Delta y} \cdot \frac{2\nu\left(\Delta x^2 + \Delta y^2\right)}{(\Delta x \Delta y)^2}\right]^{-1}$$

where $\Lambda_c$ is the Courant number, $v$ is the kinematic viscosity coefficient, $|A|$, $|B|$ are the spectral radii of the Jacobian matrices in the $x$, $y$ directions and

$$\Delta x = \sqrt{S^2_{ix} + S^2_{iy}}, \quad \Delta y = \sqrt{S^2_{jx} + S^2_{jy}},$$

where $S_{ix}$, $S_{jx}$ and $S_{iy}$, $S_{jy}$ are the $x$ and $y$ components of the normal vector mutiplied by the surface area of the surface whose normals are along $i$ and $j$ directions respectively.

Using the concepts of SLIP (Symmetric Limited Positive) scheme of Jameson [35] and flux difference splitting of Roe [25], the dissipative fluxes have been modified in the next section, in order to obtain non-oscillatory schemes.

### 5.2 Non-Oscillatory Schemes

An efficient way to high resolution without preshock oscillations, was initiated by Jameson [33]-[35], based on the concept of LED (local extremum diminishing) criterion, using flux limiters. A semi-discrete scheme is termed LED (local extremum diminishing) if the local maximum of flux does not increase and the local minimum does not decrease. It has been shown that a sufficient condition for a semi-discrete scheme to be LED is that the coefficients of the discrete approximation should be non-negative. Higher order non-oscillatory schemes that satisfy the LED property can be generated by introducing anti-diffusive terms in a controlled manner, for example, by using flux limiters. Resulting schemes are termed symmetric limited positive (SLIP) schemes [35].

For implementation of the SLIP schemes to the solution of a system of conservation laws, the idea of flux-splitting has been applied. Two different types of flux splitting techniques, viz. flux splitting by characteristic decomposition [25] and scalar splitting [33] have been considered here, applied in each coordinate direction for computation of transonic flow past airfoils. For the sake of completeness, following Jameson [35], the basic ideas in constructing SLIP schemes are presented briefly, which also explains the notations used.

Let us consider the one-dimensional scalar conservation law

$$\frac{\partial v}{\partial t} + \frac{\partial f(v)}{dx} = 0 \tag{16}$$

which may be approximated at the mesh point $i$ by the semi-discrete scheme in conservation form

$$\Delta x \frac{dv_i}{dt} + \left(h_{i+1/2} - h_{i-1/2}\right) = 0. \tag{17}$$

Here $x = i\Delta x$, $\Delta x$ denoting the mesh interval and $h_{i+1/2}$ is the numerical flux between cells $i$ and $i + 1$ . It has been established [33] that the least diffusive first order scheme that satisfies the LED property is obtained by approximating the flux as

$$h_{i+1/2} = 1/2\,(f_{i+1} + f_i) - d_{i+1/2} \tag{18}$$

where

$$d_{i+1/2} = 1/2\left|a_{i+1/2}\right| \Delta v_{i+1/2} = \alpha_{i+1/2}\,(v_{i+1} - v_i) \tag{19}$$

is a first order diffusive flux computed at cell interface $i+1/2$, as the first difference of $v$ scaled by the absolute value of the approximation of the wave speed $a(v) = \frac{\partial f}{\partial v}$.

Higher order non-oscillatory schemes may be constructed by introducing anti-diffusive terms in a controlled manner or by using flux limiters. By subtracting neighboring differences, the third order diffusive flux

$$d_{i+1/2} = \alpha_{i+1/2}\{\Delta v_{i+1/2} - 1/2(\Delta v_{i+3/2} + \Delta v_{i-1/2})\}, \tag{20}$$

where $\Delta v_{i+1/2} = v_{i+1} - Vi$ may be obtained, which produces much oscillations in the vicinity of shock waves, that can be eliminated by switching locally to first order schemes [1],[14],[40].

On the other hand, the diffusive flux Eq.(19) can be modified by the insertion of limiters so as to obtain a three point scheme with positive coefficients, which satisfy the LED criterion.

Let $L(u, v)$ be a limited average of u and v with the followingproperties:

**(P1)** L(u,v) = L(v,u)

(P2) L($\alpha$ u,$\alpha$ v) = $a$ L(u,v)

(P3) L(u,u) = u

(P4) L(u,v) = 0 if u and v have opposite signs

Properties ($P1$ - P3) are natural properties of an average. Property (P4) is needed for the construction of an LED or TVD scheme.

The diffusive flux for a scalar conservation law is then defined as

$$d_{i+1/2} = \alpha_{i+1/2}\Delta v_{i+1/2} - L\left(\alpha_{i+3/2}\Delta v_{i+3/2}, \alpha_{i-1/2}\Delta v_{i-1/2}\right)$$

The corresponding scheme is referred to as the symmetric limited positive ( SLIP) scheme.

### 5.3 Flux-Limiters

A variety of limiters $L(u, v)$ were introduced by earlier authors [29],[23],[24] which meet the requirements of the above properties. In particular, by defining

$$S(u, v) = \frac{1}{2}\{sign \mid u \mid + sign\ v \mid\} \tag{21}$$

we may easily implement any of the three well known limiters, viz.,Min-mod, Van Leer or Super-bee given

by

(i) *Min-mod*:

$$L(u,v) = S(u,v)min(|u|,|v|)$$

(ii) *Van-leer*:

$$L(u,v) = S(u,v)\frac{2|u||v|}{|u|+|v|}$$

(iii) *Super-bee*:

$$L(u,v) = S(u,v)\times$$
$$max\{min(2|u|,|v|),min(|u|,2|v|)\}$$

These are special cases of the following more general formulas :

(iv) $\alpha$-*mod*:

$$L(u,v) = S(u,v)\frac{(1+\alpha)|u||v|}{max(|u|,|v|)+\alpha min(|u|,|v|)}$$

(v) $\alpha$-*bee*:

$$L(u,v) — S(u,v)\times$$
$$max\{min(\alpha|u|,|v|),min(|u|,\alpha|v|)\}$$

(vi) $\alpha$-*mean*:

$$L(u,v) = S(u,v)min\left(\frac{|u+v|}{2},\alpha|u|,\alpha|v|\right)$$

Construction of diffusive flux for system of conservation laws is achieved through flux splitting [35],[25]. Three different types of flux splitting have been considered in [35]. Among these, flux- difference splitting by characteristic decomposition and scalar splitting have been implemented in the present work.

### 5.4 Flux splitting by characteristic decomposition

Roe [25] formulated flux-difference splitting by distributing the corrections due to the flux difference in each interval upwind and downwind. The difference scheme yields the symmetric limited positive (SLIP) scheme, applied to the differences of the characteristic variables. Let us introduce the flux-difference Af for system of conservation laws

$$\frac{\partial \mathbf{w}}{dt} + \frac{\partial \mathbf{f}(\mathbf{w})}{dx} = 0$$

by

$$\Delta \mathbf{f}_{i+1/2,j} = A_{i+1/2,j}\Delta \mathbf{w}_{i+1/2,j}$$

where $\Delta \mathbf{f}_{i+1/2,j} = \mathbf{f}_{i+1,j} - \mathbf{f}_{i,j}$, $\Delta \mathbf{w}_{i+1/2,j} = \mathbf{w}_{i+1,j} - \mathbf{w}_{i,j}$ and $A_{i+1/2,j}$ is the Jacobian matrix calculated with Roe averaging,

$$\bar{q} = \frac{\sqrt{\rho_{i+1,j}}q_{i+1,j} + \sqrt{\rho_{i,j}}q_{i,j}}{\sqrt{\rho_{i+1,j}} + \sqrt{\rho_{i,j}}}$$

for any quantity q representing a flow variable. A splitting according to characteristic fields is obtained by decomposing $A_{i+1/2}$ as $A_{i+1/2} = T\Lambda T^{-1}$ where the columns of $T$ are the eigenvectors of $A_{i+1/2}$ and A is a diagonal matrix of the eigenvalues. Then the first order diffusive flux vector which correspond to a pure upwind scheme is $\vec{d}_{i+1/2} = \frac{1}{2} A_{i+1/2}\Delta \mathbf{w}_{i+1/2}$ where $A_{i+1/2}| = T|\Lambda|T^{-1}$, $|\Lambda|$ being the diagonal matrix formed by the absolute values of the eigenvalues. This is known as characteristic splitting.

Defining

$$\Delta \mathbf{v}_{i+1/2,j} = T^{-1}\Delta \mathbf{w}_{i+1/2,j},$$

SLIP construction is then applied to each element of $\Delta \mathbf{v}_{i+1/2}$j. In case of scalar splitting, the value of a is the same for all the components of the flux vector.

The basic ideas of non-oscillatory schemes as summarized in the above subsections have been used for computing the modified Euler fluxes, by replacing the artificial dissipation term in Eq.(9) by the corresponding non-oscillatory dissipation term, the flux difference splitting being applied separately in each coordinate direction. The dissipation terms are different for different limiters used. The dissipation model gives smooth convergence for viscous flow.

## 6 RESULTS AND DISCUSSIONS

Several calculations using SLIP schemes with different limiters and with the flux-difference splitting scheme have been presented in Fig.2 - Fig.8. All the calculations have been performed on algebraically generated (256x61) C-grid [39]. In order to remove grid error, and the effect of approximation in the far-field boundary condition, several test runs were made on smaller size grids and finally the grids used were chosen. The computations for each airfoil shape were carried out till the average residuals reduced below the order of $10^{-4}$, which was taken as the convergence criterion. Roughly, 2000-time steps are required to reach this level of accuracy, requiring about 27-minutes of GPU time (except those computed with the flux-difference splitting schemes which require more time). All the computations have been carried out on a Digital DEC$\alpha$-3000/600 desk-top computer-system at the Mathematics Department, I.I.T., Kharagpur.

For the sake of convenience, we have referred here the solution using the Chakrabartty[15]'s-scheme as

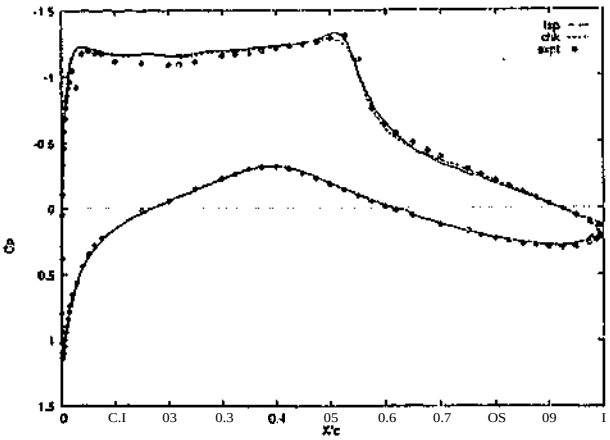

Fig. 2: Surface pressure distribution of RAE2822 airfoil for $M_\infty$ = 0.73, $a$ = 3.19 and fie = $6.5E+06$

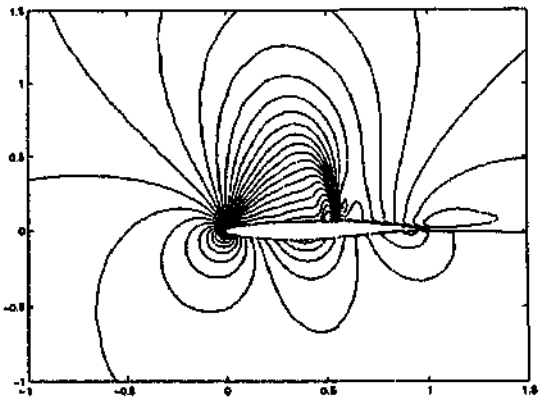

Fig.3: Pressure contours around RAE2822 airfoil for $M_\infty$ = 0.73, a = 3.19 and $Rc$ = $6.5E+06$ using 'fsp'scheme

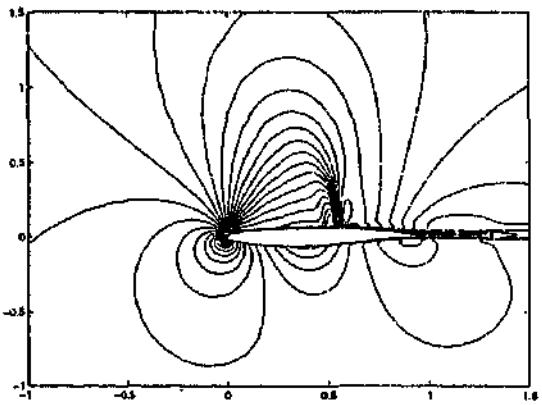

Fig.4: Mach contours around RAE2822 airfoil for $M_\infty$ = 0.73, $a$ = 3.19 and $Rc$ = $6.5E+06$ using 'fsp'scheme

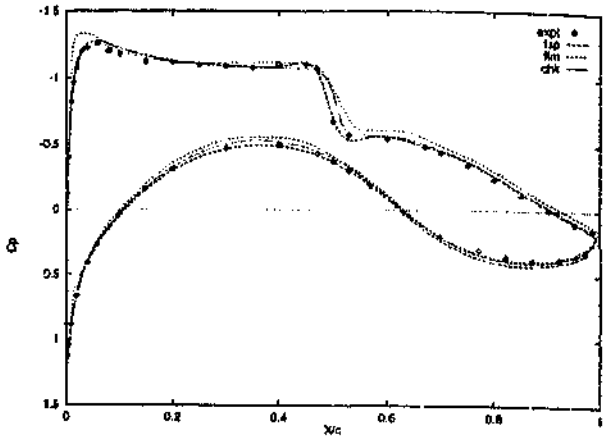

Fig.5: Surface pressure distribution of RAE5225 airfoil for $M_\infty$ = 0.737, a = 2.33 and $Rc$ = $6.0E+06$

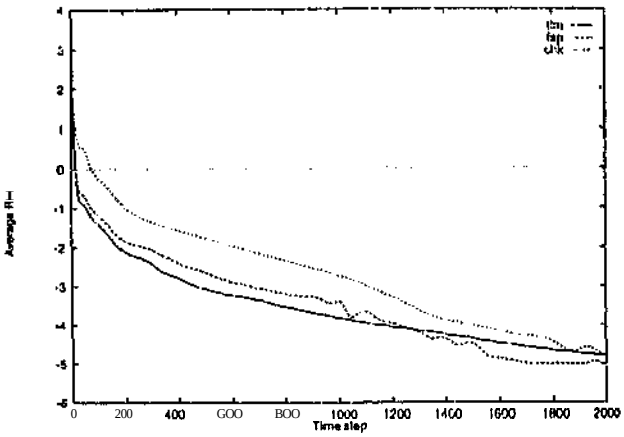

Fig.6: Curvature history of RAE5225 airfoil for $M_\infty$ = 0.737, $a$ = 2.33 and $Rc$ = $6.0E+06$

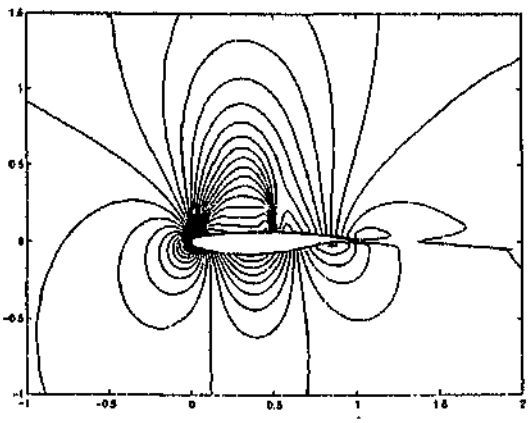

Fig.7: Pressure contours around RAE5255 airfoil for $M_\infty$ = 0.737, $\alpha$ = 2, 33 and $Rc$ = $6.0E+06$ using 'fsp'scheme

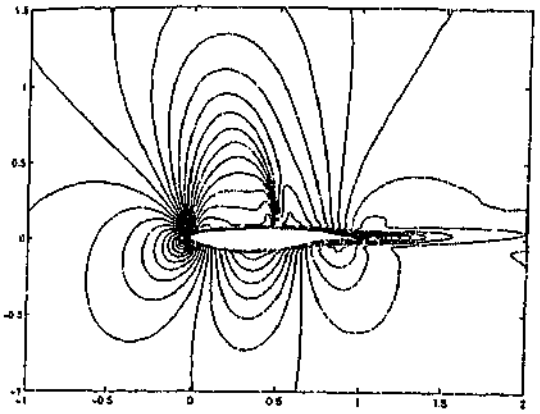

Fig.8: Mach contours around RAE5255 airfoil for $M_\infty = 0.737$, $\alpha = 2,33$ and $Rc = 6.0E+06$ using 'fsp'scheme

'chk', SLIP-schemes with scalar splitting as 'flm' and that using flux-difference splitting as 'fsp'.

For computations with chk-scheme, the parameters $k^{(2)}$ and $k^{(4)}$ for the second and fourth order dissipation have been kept fixed as $\frac{1}{2}$ and $\frac{1}{256}$ respectively. It may be noted that this choice of the parameter $k^{(4)}$ gives results which show best agreement with the experimental values. In fact, the results depend more or less strongly on the values of these parameters, which provided initial motivation for the present study.

The first example computed is that of steady-state flow for a RAE2822 airfoil at $M_\infty = 0.73$, a = 3.19° and $Re$ - $6.5E$ + 6. Fig.2 shows the $Cp$ distributions of this case where very good agreement may be noted with the fsp(LED) computations. Fig.3 and Fig.4 show the pressure contour and the Mach contour distributions for this case. The second example considered here is that of flow past a RAE5225 airfoil with $M_\infty = 0.737$, $a = 2.33°$ and $Re = 6.0E+6$. Fig.5 shows the $C_p$ distributions of this case. Here also, the results of fsp(LED) scheme show very good agreement with experimental results [43],[44]. For computing the scalar-split flm values, the $\alpha$-mod limiter has been chosen with the value of the limiter parameter equal to 3.5.

Figures 7 and 8 show the pressure and the Mach contour distributions for this case using the fsp scheme. In Fig.6 a typical convergence history has been shown where $log\left(\frac{\partial f}{\partial t}\right)$ has been plotted against the number of time steps. Convergence to a steady state has been achieved. Table-1 shows the comparison of different aerodynamic forces obtained by the present schemes under study for the two airfoils with the experimental results [42],[43],[44]. Here also, the results obtained by fsp scheme shows much improvement over chk scheme with repect to the experimental results.

## 7 CONCLUSION

The choice of artificial dissipation is very important in resolving the viscous flow phenomena properly. This plays a great role in the convergence and stability of the flow in supersonic region. Like inviscid transonic flow, for viscous transonic flow also Non-Oscillatory schemes can resolve shocks better at a reasonable computational cost . Experience with various examples computed and comparison with other theoretical and experimental results indicate that the present method is quite satisfactory.

## REFERENCES

[1] A. Jameson, W. Schmidt and E. Turkel, Numerical solutions of the Euler equations by finite volume methods using Runge-Kutta time stepping schemes, AIAA Paper 81-1259,1981.

[2] R. H. Ni, A multiple grid scheme for solving the Euler equations, AIAA J., 20 (1982)1565-1571.

[3] M. G. Hall, Cell vertex multigrid scheme for solution of the Euler equations, RAE-TM-Aero 2029.Proc. of Conf. on Num. Methods for Fluid dynamics Univ. of Reading, UK. April 1-5 (1985). IMA Conf. series, Oxford Univ. Press.

[4] A. Jameson and T. Baker, Solution of the Euler equations for complex configurations, Proc. AIAA 6th Computational Fluid Dynamics Conference, Danvers, 1983, pp. 293-302.

[5] T. H. Puliam and J. L. Steger, Recent improvements in efficiency, accuracy and convergence for implicit approximate factorization algorithms, AIAA Paper 85-0360, AIAA 23rd Aerospace Sciences Meeting, Reno, January 1985.

[6] R. M. Beam and R. F. Warming, An implicit factored scheme for the compressible Navier-Stokes equations, AIAA J. 16 (1978)393-402.

[7] R. M. Beam and R. F. Warming, Implicit Numerical Methods for Compressible Navier-Stokes and Euler Equations, Lecture Notes for Computational Fluid Dynamics, Von Karman Institute for Fluid Dynamics, March 29 - April 2, 1982, Rhode-Saint-Genêse, Belgium.

[8] L. Martenelli and A. Jameson, Validation of a multigrid method for the Reynolds averaged equations, AIAA Paper 88-0414, January 1988.

[9] R. W. MacCormack,Current status of numerical solutions of the Navier-Stokes equations, AIAA paper 85-0032, AIAA 23rd Aerospace Sciences Meeting, Reno, January 1985.

| airfoil | scheme | $M_\infty$ | $a$ | Re | CL | CD | CM |
|---|---|---|---|---|---|---|---|
| RAE2822 | Expt | 0.73 | 3.19 | 6.5E+06 | 0.803 | 0.0168 | -0.099 |
| | LED(fsp) | 0.73 | 3.19 | 6.5E+06 | 0.8827 | 0.0148 | -0.0892 |
| | chk | 0.73 | 3.19 | 6.5E+06 | 0.8449 | 0.0168 | -0.0876 |
| RAE5225 | Expt | 0.737 | 2.33 | 6.0E+06 | 0.6590 | 0.01292 | -0.0832 |
| | LED(flm) | 0.737 | 2.33 | 6.0E+06 | 0.6546 | 0.0117 | -0.0883 |
| | TVD(fsp) | 0.737 | 2.33 | 6.0E+06 | 0.6911 | 0.0099 | -0.0939 |
| | chk | 0.737 | 2.33 | 6.0E+06 | 0.6701 | 0.0118 | -0.0921 |

Table 1: Comparison of lift, drag and moment coefficients of different airfoils using different schemes with experiments.

[10] W. Kordulla, The Computation of Three Dimensional Viscous Transonic Flows with Separation, Lecture Notes in Physics,**218**,Springer-Verlag (1984)320-326.

[11] R. C. Swanson and E. Turkel, A Multistage Time-Stepping Scheme for the Navier-Stokes Equations, AIAA-85-0035.AIAA 23rd Aerospace Science meeting, June 14-17, Reno, Neveda,1985.

[12] B. Muller, Navier-Stokes Solution of Laminar Transonic Flow Over a NACA0012 Airfoil, FFA report-140,1986.

[13] S. K. Chakrabartty, Numerical solution of two-dimensional Navier-Stokes equations by finite-volume method, National Aerospace Laboratories Report PD-FM 8726, Bangalore, India 1987.

[14] S. K. Chakrabartty, Numerical solution of Navier-Stokes equations for two-dimensional viscous compressible flows, AIAA Journal 27 (1989), 843-844.

[15] S. K, Chakrabartty, A finite-volume nodal point scheme for solving two-dimensional Navier-Stokes equations, Acta Mechanica, 84 (1990) 139-153.

[16] S. K. Chakrabartty, Vertex-based finite volume solution of the two-dimensional Navier-Stokes equations, AIAA Journal, 28 (1990) 1829-1831.

[17] S. K. Chakrabartty and K. Dhanalakshmi, Computation of transonic flows with shock induced separation using algebraic turbulence models, AIAA Journal, **33** (1995)1979-1981.

[18] R. Radespiel,A Cell-Vertex Multigrid Method for the Navier-Stokes Equations, NASA TH 101557, 1989.

[19] S. K. Chakrabartty and K. Dhanalakshmi,Navier-Stokes analysis of Korn aerofoil, Acta Mechanica, **118** (1996) 235-239.

[20] S. K. Chakrabartty, Some results of compressible viscous flows past aerofoils using a modified time step for stability, NAL-PD-CF-9129 (1991), Bangalore.

[21] R. D. Richtmyer and K. W. Morton, Difference Methods for Initial Value Problems,Second Edition, Interscience Publishers, New-York, 1967.

[22] P.D.Lax, Hyperbolic Systems of Conservation Laws and the Mathematical Theory of Shock Waves, SIAM Region. Ser. Appl. Math. Vol.11, *SIAM Philadelphia,* Pa 1973.

[23] J. P. Boris and D. L. Book,Flux corrected transport I: SHASTA - A Fluid Transport Algorithm that Works, J. Comp. Physics, 31 (1973) 38-69.

[24] B. Van Leer,Towards the ultimate conservative difference scheme V : a second order sequel to Godunov's method, J. Comp. Phys.,**32** (1979) 101-136.

[25] P. L. Roe, Approximate Riemann solvers, parameter vectors and difference schemes, J. *Comp. Phys.* **43** (1981)357-372.

[26] P. L. Roe, Some contributions to the modelling of discontinuous flows, Lectures in Applied Mathematics, Vol. 22 (Amer. Math. Soc., Providence, R.I., 1985)

[27] A. Harten, High resolution schemes for hyperbolic conservation laws, *J. Comp. Phys.***49**(1983)357-393.

[28] S. Osher and F. Solomon, Upwind difference schemes for hyperbolic systems of conservation laws, Mathematics and Computing, 38(1982)339-374.

[29] S. Osher, Riemaim solvers, the entropy condition and difference approximations, *SIAM* J. *Num. Anal.* 21(1984)217-235.

[30] p. K. Sweby, High resolution schemes using flux limiters for hyperbolic conservation laws, *SIAM J. Num. And.11* (1984)995-1011.

[31] H. C. Yee, Construction of explicit and implicit symmetric TVD-schemes and their applications, J. Comp. Phys.,68 (1987)151-179.

[32] H. C. Yee, A Class of High-Resolution Explicit and Implicit Shock-Capturing Methods, NASA TM 101088, Feb. 1989. Also, Von Karman Institute for Fluid Dynamics Lecture Series 1989-04, Computational Fluid Dynamics, March 6-10, 1989, Rhode-St-Genèse, Belgium.

[33] A. Jameson, A non-oscillatory shock capturing scheme using flux limited dissipation, Lectures in Applied Mathematics, Ed.: B.E.Engquist, S.Osher, and R.C.J. Sommerville, Amer. Math. Soc.,Part-l,22:354-370,1985.

[34] A. Jameson, Success and Challenges in Computational Aerodynmics, AIAA paper 87-1184.

[35] A. Jameson, Artificial diffusion, upwind biasing, limiters and their effect on accuracy and multigrid convergence in transonic and hypersonic flows, *AIAA-93-3359*, 11-th AIAA Computational Fluid Dynamics Conference, Orlando, FL, July 6-9,1993.

[36] S. Tatsumi, L. Martinelli and A. Jameson, Design, implementation and validation of Flux Limited schemes for the solution of the compressible Navier-Stokes equations, 32nd Aerospace Sciences Meeting of Exhibit, January 10-13, 1994, Reno, NV.

[37] H. C. Yee, G. H. Klopfer and J. L. Montagne, High-Resolution shock-capturing schemes for inviscid and viscous hypersonic flow, J. Comp. Phys.,88(1990)31-61.

[38] B. S. Baldwin and H. Lomax, Thin Layer Approximation and Algebraic Model for Separated Turbulent Flows, AIAA Paper 78-257. 1978.

[39] R. K. Jain, Grid generation about an aerofoil by the algebraic equation method, DFVLR-IB-129-83/90, Germany.

[40] R. C. Swanson and E. Turkel, On central difference and upwind schemes, J. Comp. Phys.,101 (1992) 297-306.

[41] J. L. Steger and R. Warming, Flux vector splitting of the inviscid gasdynamic equations with application to finite difference methods, J.Comp.Phys.,40(1981)263-293.

[42] P.H. Cook, M.A. McDonald and M.C.P. Firmin, Aerofoil RAE2822 - Pressure Distributions and Boundary Layer and Wake Measurements, AGARD - AR - 138, 1979.

[43] P.R. Ashill, R.F. Wood and D.J. Weeks, An Improved Semi-inverse Version of the Viscous Garabedian and Korn Method (VGK), RAE Tech. Rep. 87002, Jan. 1987.

[44] P.R. Ashill, D.J. Weeks and J.L. Fulker, Wind Tunnel Experiments on Aerofoil Models for the Assessment of Computational Flow Methods, AGARD CP 437, Dec. 1988.